

Reactivity of Octahedral η^1 -Allenyl Iridium toward Hard Nucleophiles[†]

Ray-Hsi Hsu, Jwu-Ting Chen,* Gene-Hsiang Lee, and Yu Wang

Department of Chemistry, National Taiwan University, Taipei, Taiwan 106, Republic of China

Received April 3, 1996[⊗]

A labile octahedral (η^1 -allenyl)iridium complex, (*OC*-6-42)-Ir(Cl)(PPh₃)₂(OTf)(CO)(η^1 -CHCCH₂) (**2a**), undergoes regioselective addition with water or alcohol at the allenyl central carbon to generate the (η^3 -2-hydroxyallyl) and (η^3 -2-alkoxyallyl)iridium complexes {Ir(Cl)(PPh₃)₂(CO)[η^3 -CH₂C(OR)CH₂]}(OTf) (R = H (**3**), Me (**4a**), Et (**4b**)), respectively. The complex **3** and the η^3 -oxa-TMM species Ir(Cl)(PPh₃)₂(CO)[η^3 -CH₂C(O)CH₂] (**5**) constitutes a conjugate acid–base pair. Hydrolysis of the η^3 -alkoxyallyl complexes yields **3**, which further transforms into the carbon-bound iridium enolate (*OC*-6-52)-{Ir(Cl)(PPh₃)₂(OH₂)(CO)[η^1 -CH₂C(O)CH₃]}(OTf) (**6**). The reaction of **2a** with ammonia results in the substitution of NH₃ for the triflate ligand instead of hydroamination to the allenyl ligand. The construction of the C–N bond, however, is alternatively achieved by replacing the alkoxy group in **4a** or **4b** with the amino group, leading to the formation of the N-protonated and N-alkylated η^3 -aza-TMM iridium {Ir(Cl)(PPh₃)₂(CO)[η^3 -CH₂C(NR₂)CH₂]}(OTf) (R = H (**7a**), Et (**7b**)).

Introduction

Since the first η^1 -allenyl complex was prepared,⁴ the chemistry of transition-metal allenyl complexes has been continuously attracting research interest for more than two decades. The greatest portion of research in this area has focused on the synthetic aspect. Various features of the allenyl ligands have been developed.^{5,8} Nevertheless, the reactivity of the (η^1 -allenyl)metal complexes has been relatively overlooked. Recent studies on metal allenyl species reveal that the organic ligands are subject to regioselective nucleophilic addition.⁶ Our previous study on a square-planar (η^1 -allenyl)platinum complex indicates that the η^1 -allenyl ligand is linear and undergoes hydroamination.³ It has also been noted that the η^1 -allenyl ligand appears to be inert to external attack by nucleophiles.⁷ We propose that it may need the precoordination of the nucleophile

to facilitate its addition to the η^1 -allenyl ligand. Comparing the η^1 -allenyl complexes with a class of newly developed cationic η^3 -propargyl/ η^3 -allenyl complexes,⁸ we find that the η^1 -allenyl species react with nucleophiles at a slower pace; the reaction scope is also less general. The mechanistic rationale for such a discrepancy still remains elusive and calls for more thorough investigation.

In this work, we report the preparation of a labile octahedral η^1 -allenyl complex of iridium, (*OC*-6-42)-Ir(Cl)(PPh₃)₂(OTf)(CO)(η^1 -CHCCH₂), and its reactions with hard nucleophiles have been studied. We turn to such a system not only because that changing metal will allow us to examine the generality of the reactivity of the η^1 -allenyl group in nucleophilic addition but also because we wish to understand how the coordination affects the reactivity. It is found that the six-coordinate (η^1 -allenyl)iridium complex undergoes the regioselective addition of water or alcohol to form the η^3 -hydroxyallyl and η^3 -alkoxyallyl complexes, respectively. In contrast, reactions with better nucleophiles such as ammonia and amine derivatives result in substitution for the triflate ligand instead. Such results suggest that both the coordinating ability and the acidity of the nucleophile should be crucial to the addition of (η^1 -allenyl)iridium. The products of hydroamination are alternatively formed from the unusual substitution reactions of the η^3 -alkoxyallyl group with ammonia or amine at the central carbon.

[†] Based on the M.S. thesis of R.-H.H., National Taiwan University, 1994. The η^3 -Oxatrimethylenemethane complex M[η^3 -CH₂C(O)CH₂] is abbreviated as η^3 -oxa-TMM;¹ η^3 -aza-TMM stands for the η^3 -azatrimethylenemethane complex M[η^3 -CH₂C(NR)CH₂];² M[η^3 -CH₂C(NH₂)CH₂] is referred to as N-protonated η^3 -azatrimethylenemethane; M[η^3 -CH₂C-(NR'R')CH₂] (R, R' = alkyl, aryl) is N-alkylated (or -arylated) η^3 -azatrimethylenemethane.³ The prefix *OC*-6-42 follows IUPAC nomenclature from: *Nomenclature of Inorganic Chemistry: Recommendations*, Leigh, G. J., Ed.; Blackwell: Oxford, U.K., 1990.

[⊗] Abstract published in *Advance ACS Abstracts*, February 1, 1997.

(1) Jones, M. D.; Kemmitt, R. D.; Fawcett, J.; Russel, D. R. *J. Chem. Soc., Chem. Commun.* **1986**, 427.

(2) (a) Ohe, K.; Matsuda, H.; Morimoto, T.; Ogoshi, S.; Chatani, N.; Murai, S. *J. Am. Chem. Soc.* **1994**, *116*, 4125. (b) Baize, M. W.; Plantevin, V.; Gallucci, J. C.; Wojcicki, A. *Inorg. Chim. Acta* **1995**, *235*, 1.

(3) Chen, J.-T.; Huang, T.-M.; Cheng, M.-C.; Lin, Y.-C.; Wang, Y. *Organometallics* **1992**, *11*, 1761.

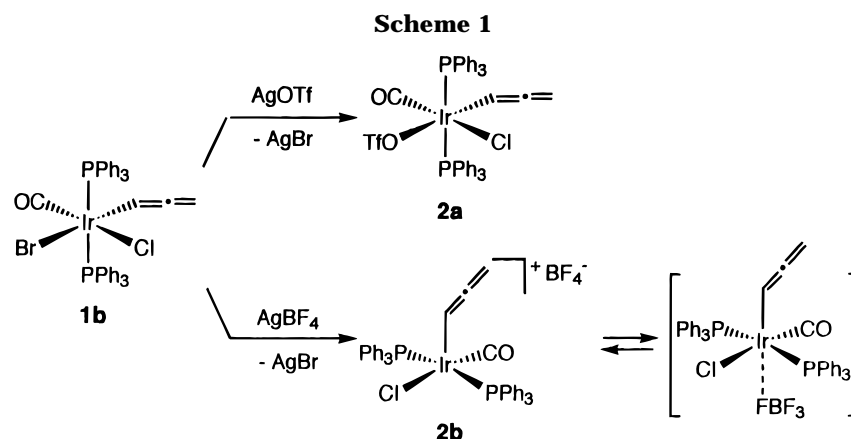
(4) Collman, J. P.; Cawse, J. N.; Kang, J. W. *Inorg. Chem.* **1969**, *8*, 2574.

(5) (a) Wojcicki, A. *Adv. Organomet. Chem.* **1974**, *12*, 31. (b) Casey, C. P.; Austin, E. A. *J. Am. Chem. Soc.* **1988**, *110*, 7106. (c) Young, G. H.; Wojcicki, A.; Calligaris, M.; Nardin, G.; Bresciani Pahor, N. *J. Am. Chem. Soc.* **1989**, *111*, 6890. (d) Wojcicki, A.; Shuchart, C. E. *Coord. Chem. Rev.* **1990**, *105*, 35. (e) Wouters, J. M.; Klein, R. A.; Elsevier, C. J.; Zoutberg, M. C.; Stam, C. H. *Organometallics* **1993**, *12*, 3864. (f) Wouters, J. M.; Klein, R. A.; Elsevier, C. J.; Häming, L.; Stam, C. H. *Organometallics* **1994**, *13*, 4586.

(6) Carty, A. J. *Adv. Organomet. Chem.* **1995**, *12*, 31 and references therein.

(7) Huang, T.-M.; Hsu, R.-H.; Yang, C.-S.; Chen, J.-T.; Lee, G.-H.; Wang, Y. *Organometallics* **1994**, *13*, 3657.

(8) (a) Krivykh, V. V.; Taits, E. S.; Petrovskii, P. V.; Struchkov, Y. T.; Yanovskii, A. I. *Mendeleev Commun.* **1991**, 103. (b) Casey, C. P.; Yi, C. S. *J. Am. Chem. Soc.* **1992**, *114*, 6597. (c) Casey, C. P. *Science* **1993**, *259*, 1552. (d) Blosser, P. W.; Schimpff, D. G.; Gallucci, J. C.; Wojcicki, A. *Organometallics* **1993**, *12*, 1993. (e) Blosser, P. W.; Gallucci, J. C.; Wojcicki, A. *J. Am. Chem. Soc.* **1993**, *115*, 2994. (f) Stang, P. J.; Crittall, C. M.; Arif, A. M. *Organometallics* **1993**, *12*, 4799. (g) Huang, T.-M.; Chen, J.-T.; Lee, G.-H.; Wang, Y. *J. Am. Chem. Soc.* **1993**, *115*, 1170. (h) Baize, M. W.; Furilla, J. L.; Wojcicki, A. *Inorg. Chim. Acta* **1994**, *233*, 1. (i) Plantevin, V.; Blosser, P. W.; Gallucci, J. C.; Wojcicki, A. *Organometallics* **1994**, *13*, 3651. (j) Baize, M. W.; Blosser, P. W.; Plantevin, V.; Schimpff, D. G.; Gallucci, J. C.; Wojcicki, A. *Organometallics* **1996**, *15*, 164. (k) Tsai, F.-Y.; Hsu, R.-H.; Chen, J.-T.; Huang, T.-M.; Lee, G.-H.; Wang, Y. *J. Organomet. Chem.* **1996**, *520*, 85.



Results and Discussion

Synthesis and Characterization of (η^1 -Allenyl)-iridium Complexes. (*OC*-6-43)-Ir(Cl)₂(PPh₃)₂(CO)(η^1 -CHCCH₂) (**1a**) and (*OC*-6-54)-Ir(Br)(Cl)(PPh₃)₂(CO)(η^1 -CHCCH₂) (**1b**) were prepared according to the literature method with use of oxidative addition.⁴ The compositions of **1a** and **1b** are indicated by mass spectrometry and the elemental analysis, and the structures are supported by spectroscopy and the ensuing chemical transformations. Unlike the square-planar *trans*-Pt(Br)(PPh₃)₂(η^1 -CHCCH₂), which reacts with equimolar amounts of amine to form the N-alkylated (or arylated) η^3 -aza-TMM species at 25 °C, there is no reaction between complexes **1** and equimolar amine even at 60 °C. This result indicates that the linear η^1 -allenyl ligand indeed does not undertake direct external nucleophilic attack. The octahedral **1a** and **1b**, which contain no labile ligand, are probably inert to the substitution of amine and thus leave no chance for subsequent addition of the allenyl group. In order to pursue the support for this assertion, we prepared a triflate derivative of the allenyliridium complex for further study.

Treatment of **1b** with equimolar amounts of AgOSO₂CF₃ leads to the formation of the triflate allenyl complex (*OC*-6-42)-Ir(Cl)(PPh₃)₂(OTf)(CO)(η^1 -CHCCH₂) (**2a**). The reaction of **1a** and AgOTf was complicated, although the triflate derivative was indeed detected with NMR techniques. The solid form of **2a** is stable under a dry nitrogen atmosphere but tends to deteriorate in air. It also suffers decomposition in solution rapidly. We did not attempt to identify the decomposed residue. The linear η^1 -allenyl ligand in **2a** is soundly evidenced by the ¹H NMR signals at δ 3.93 (H_γ) and 5.66 (H_α) in a ratio of 2:1 and the ¹³C NMR signals at δ 55.2 (C_α), 72.4 (C_γ), and 205.4 (C_β). The triflate group of **2a** exhibits its infrared absorptions at 1001, 1230, and 1317 cm⁻¹, suggesting that such a triflate ion is in a coordinating mode rather than acts as a counteranion.⁹ Other spectral data for **2a** such as infrared absorptions of ν_{CO} and $\nu_{\text{C}=\text{C}}$, and ³¹P NMR are comparable to those of **1b**. The molar conductivities of **1b** and **2a** measured in noncoordinating CH₂Cl₂ at 25 °C are 0.79 and 3.35 cm² equiv⁻¹ Ω⁻¹, respectively. These data are substantially smaller than the value 10.30 cm² equiv⁻¹ Ω⁻¹ due to the ionic complex **7a** (vide supra) measured under the same conditions. Accordingly, **2a** is likely a neutral

species, although partial dissociation of triflate from **2a** cannot be excluded.

In order to know whether **2a** could release the triflate ion to form a η^3 -propargyl/ η^3 -allenyl species, we have deliberately examined the reaction of **1b** with AgBF₄ in CDCl₃ at -40 °C. Within the first NMR measurement, an intermediate **2b** that clearly contains a η^1 -allenyl ligand is detected. The sharp singlet in its ¹⁹F NMR at -40 °C suggests that the BF₄⁻ ion may be free or may be in a rapidly exchanging process in solution.¹⁰ Complex **2b** is thus considered to be either the cationic pentacoordinate species [Ir(Cl)(PPh₃)₂(CO)(η^1 -CHCCH₂)]⁺(BF₄⁻) or a pseudooctahedral complex. The similarity of the NMR data between **2a** and **2b** suggests that **2b** may be in a tetragonal-pyramidal environment (Scheme 1). Isolation of **2b** is not feasible, because it decomposes either in solution or upon recrystallization. Therefore, **2a** has been used as the starting species throughout this study.

Addition of Water and Alcohol to Ir(Cl)(PPh₃)₂(OTf)(CO)(η^1 -CHCCH₂) (2a**).** In contrast to the halo species **1a** and **1b**, the labile triflate complex **2a** is subject to nucleophilic addition, again indicating that the coordination of nucleophile is crucial to the addition process. The reaction of **2a** with an equimolar amount of water at 0 °C under nitrogen readily generates the cationic (hydroxyallyl)iridium species {Ir(Cl)(PPh₃)₂(CO)[η^3 -CH₂C(OH)CH₂]}⁺(OTf)⁻ (**3**). In the ¹H NMR spectrum of **3**, a broad peak at δ 11.5 is ascribed to the hydroxyl proton and the signals at δ 2.96 and 3.78 are assigned to the anti and syn hydrogens of η^3 -allyl, respectively. The characteristic ¹³C NMR data for the terminal and central carbon atoms of the allyl ligand are found at δ 50.4 and 168.3.

Single crystals of **3** are grown from CH₂Cl₂ and Et₂O cosolvent. The X-ray diffraction unequivocally confirms the assigned structure of **3**, which is shown in Figure 1. Complex **3** has a slightly distorted trigonal bipyramidal geometry. The chloride and carbonyl ligands are at the axial positions. The allyl moiety in a η^3 mode sits in a tilted manner at the equatorial position. The C3 atom approaches the metal toward the carbonyl side. The four-member framework of MC₃ folds along the axis defined by the C2 and C4 atoms with the C2-C3-C4 and C2-Ir-C4 planes constituting a dihedral angle of 58(1)°. As a result, the allyl central carbon is substantially more distant from the iridium center than the two

(9) (a) Blake, D. M. *J. Chem. Soc., Chem. Commun.* **1974**, 815. (b) Lawrence, G. A. *Chem. Rev.* **1986**, 86, 17.

(10) Smith, G.; Cole-Hamilton, D.-J.; Gregory, A. C.; Gooden, N. G. *Polyhedron* **1982**, 1, 97.

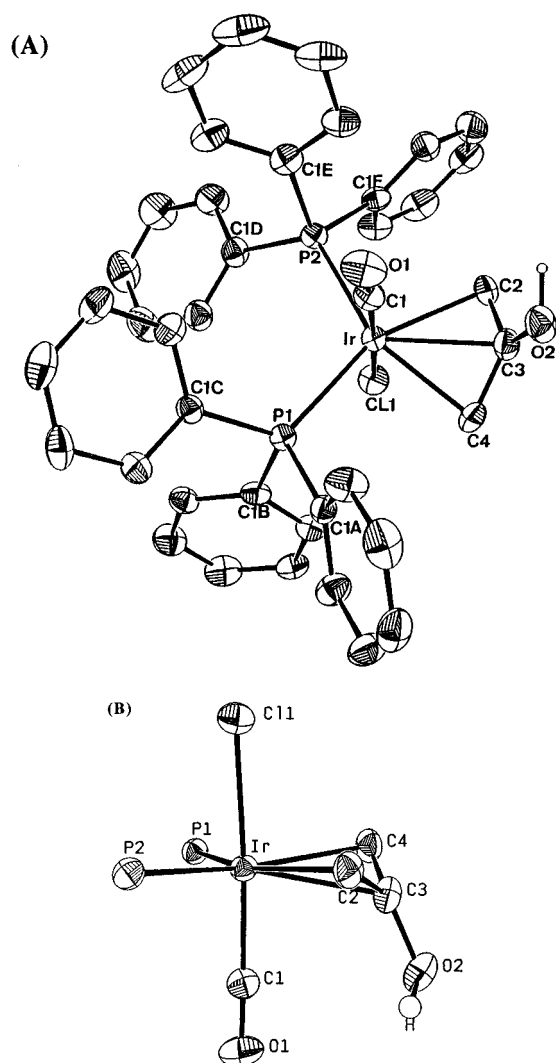
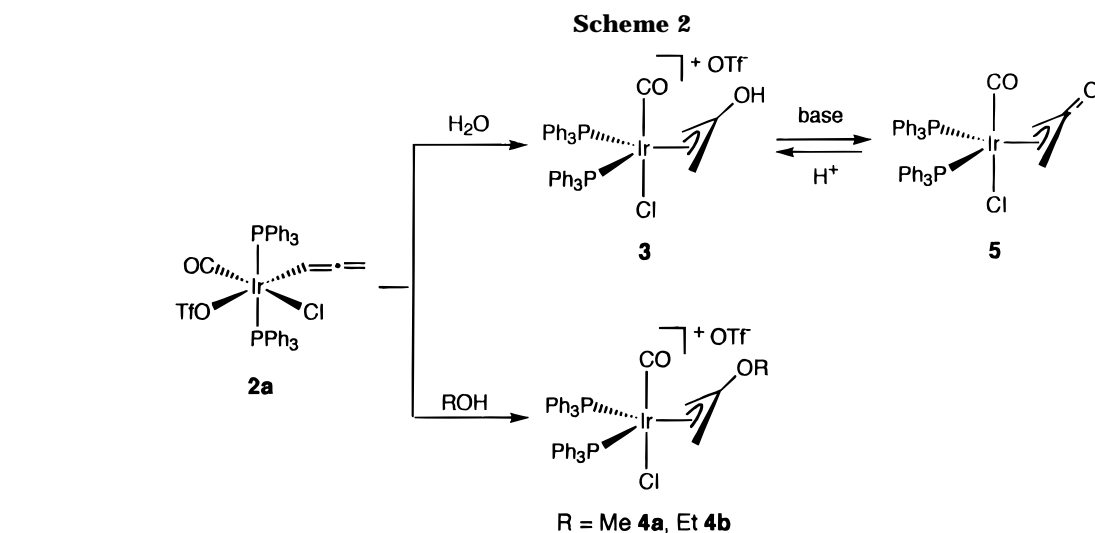


Figure 1. ORTEP drawing of the cation of **3**, $\{\text{Ir}(\text{Cl})(\text{PPh}_3)_2(\text{CO})[\eta^3\text{-CH}_2\text{C}(\text{OH})\text{CH}_2]\}^+$. All hydrogen atoms are omitted for clarity.

allyl terminal carbons, with $D(\text{Ir}-\text{C}3) = 2.34(1) \text{ \AA}$, $D(\text{Ir}-\text{C}2) = 2.22(1) \text{ \AA}$, and $D(\text{Ir}-\text{C}4) = 2.23(1) \text{ \AA}$. The hydroxy group attaches to the central carbon C3 with $D(\text{C}3-\text{O}2) = 1.33(1) \text{ \AA}$, which is rather short in comparison with the platinum analogue.⁷ The hydroxy hydrogen is arbitrarily located at a fixed distance of 0.96 Å from the oxygen atom.

The complex **2a** also reacts with alcohol in a similar manner to yield the first iridium complexes with η^3 -2-alkoxyallyl ligands, $\{\text{Ir}(\text{Cl})(\text{PPh}_3)_2(\text{CO})[\eta^3\text{-CH}_2\text{C}(\text{OR})\text{CH}_2]\}(\text{OTf})$ (R = Me (**4a**), Et (**4b**)), in good yields (Scheme 2). The complexes **4a** and **4b** decompose in air even in the solid state. Their elemental data are not satisfactory. We have mainly characterized **4a** and **4b** by spectroscopic methods. The FAB mass analysis of **4a** and **4b** gives the molecular weights of the cations. The ¹H NMR signals of anti and syn hydrogens are detected at δ 3.16 and 3.60 for **4a** and δ 3.15 and 3.58 for **4b**. The ¹³C NMR resonances of the terminal and central carbon atoms of the allyl ligand are observed at δ 48.8 and 168.1 for **4a** and δ 49.0 and 167.9 for **4b**, respectively. These data are comparable to those for **3**. The methoxy protons of **4a** appear at δ 3.78 and at δ 1.34 and 3.97 with a 3:2 ratio of integration for the ethoxy protons of **4b**. Other spectral data also closely resemble those of **3**. Therefore, the alkoxyallyl complexes **4a** and **4b** are thought to have the similar structural features similar to those of **3**. Scheme 2 illustrates the convenient synthesis of substituted (η^3 -allyl)iridium species by constructing the C–O bond regioselectively at the allenyl central carbon. The chemical discrepancy between **1a**, **1b**, and **2a** toward the nucleophiles is attributed to the difference in the ligand lability.

Hydrolysis of Hydroxyallyl and Alkoxyallyl Complexes of Iridium. The hydroxy group of **3** is moderately acidic. Complex **3** can be transformed into the neutral η^3 -oxa-TMM species $\text{Ir}(\text{Cl})(\text{PPh}_3)_2(\text{CO})[\eta^3\text{-CH}_2\text{C}(\text{O})\text{CH}_2]$ (**5**) by treating with base. Addition of benzoic acid or stronger acids to **5** yields **3**. However, acetic acid fails to protonate **5**. Exposing complex **4a** or **4b** to air leads to the transformation into the hydroxyallyl complex **3** (vide supra) accompanied by the formation of the corresponding alcohol. Complex **3** further slowly transforms into the cationic (enolato)iridium species $(\text{OC-6-52})\text{-}\{\text{Ir}(\text{Cl})(\text{PPh}_3)_2(\text{H}_2\text{O})(\text{CO})[\eta^1\text{-CH}_2\text{C}(\text{O})\text{CH}_3]\}(\text{OTf})$ (**6**) (Scheme 3). The structure of **6** has been determined by X-ray diffraction and is shown in Figure 2. It shows that **6** is six-coordinate and the enolate ligand is in a carbon-bound keto form. An aquo ligand is located cis to the enolate and trans to the carbonyl. The two phosphines of **6** are disposed at trans positions.

The formation of **6** is presumably due to the reaction of **3** with water. The entering water can facilitate the

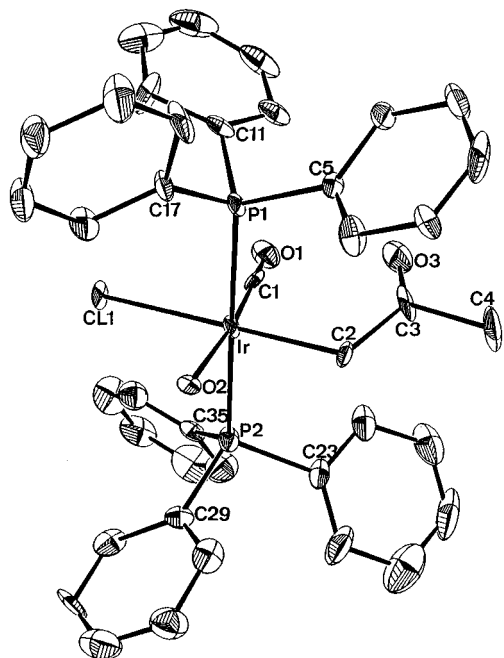
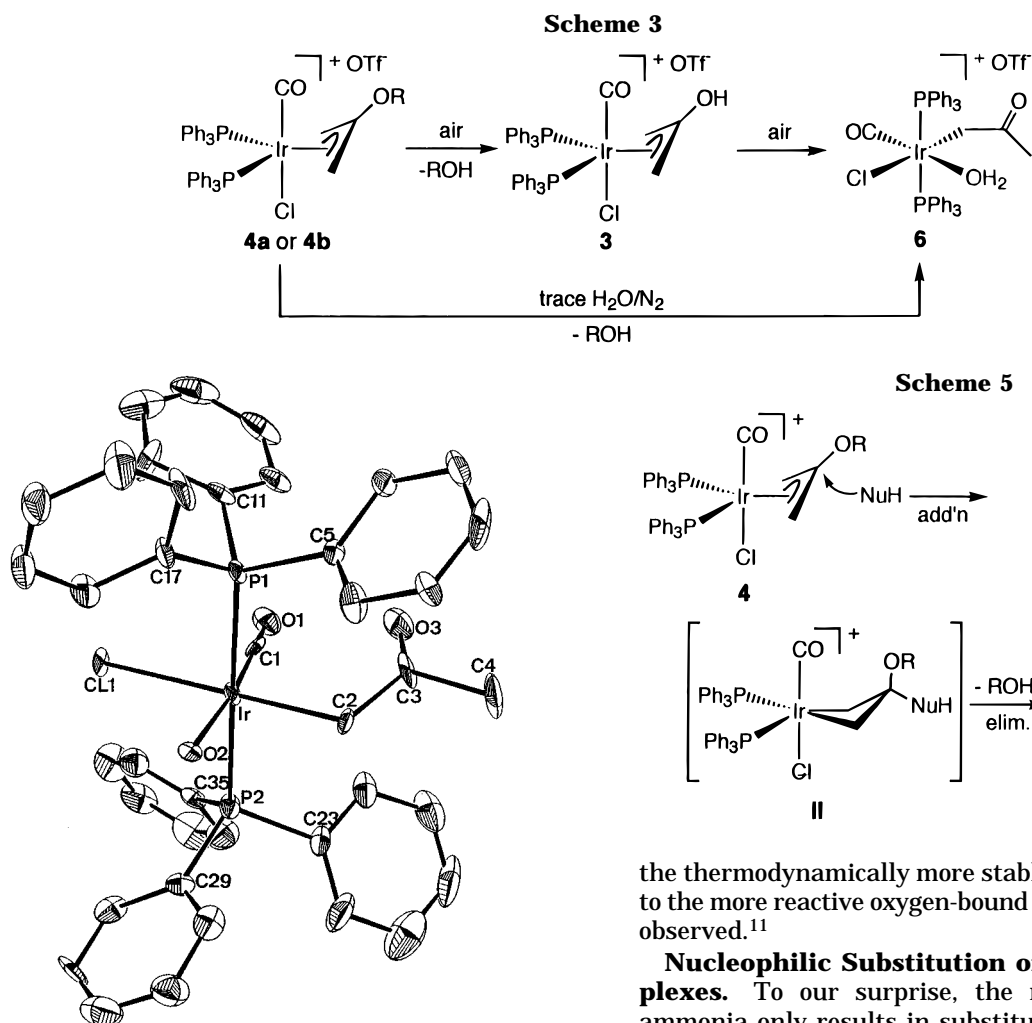
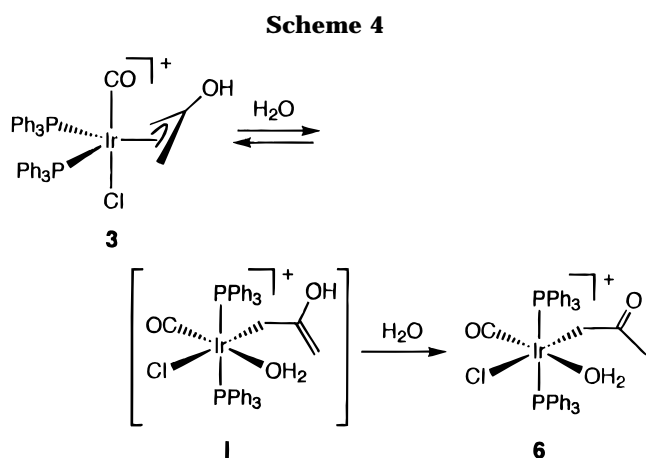


Figure 2. ORTEP drawing of the cation of **6**, $(OC-6-52)\text{-}\{\text{Ir}(\text{Cl})(\text{PPh}_3)_2(\text{H}_2\text{O})(\text{CO})[\eta^3\text{-CH}_2\text{C}(\text{O})\text{CH}_3]\}^+$. All hydrogen atoms are omitted for clarity.



conversion of **3** to the η^1 -enol intermediate **I** followed by a proton transfer to generate **6** (Scheme 4). The hydrolysis of **3** to **I** is likely reversible. When a solution of **4a** or **4b** is present with insufficient water, complex **6** is formed at a much slower pace at the expense of **4a** or **4b**, but without the detection of **3**. Our attempt to establish the "aldol reaction" by reacting the (enolato)iridium species **6** or the (hydroxyallyl)iridium complex **3** with either aldehyde or silyl halide has not been successful. Although complex **6** contains a weak aquo ligand cis to the enolate ligand, tautomerization from

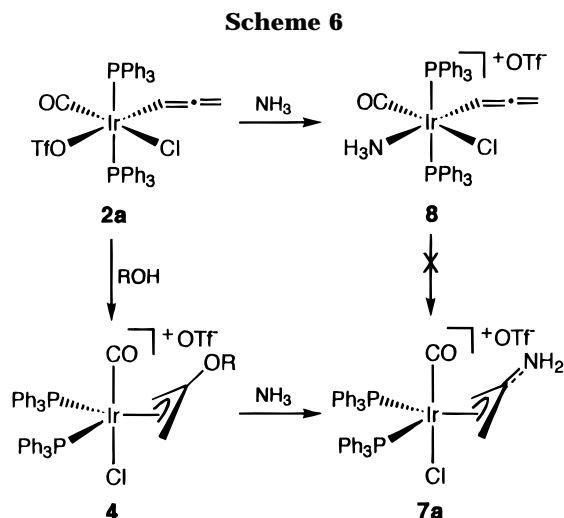
the thermodynamically more stable carbon-bound form to the more reactive oxygen-bound form has not yet been observed.¹¹

Nucleophilic Substitution of Alkoxyallyl Complexes. To our surprise, the reaction of **2a** with ammonia only results in substitution, yielding $(OC-6-42)\text{-}\{\text{Ir}(\text{Cl})(\text{PPh}_3)_2(\text{NH}_3)(\text{CO})(\eta^1\text{-CHCCH}_2)\}(\text{OTf})$ (**8**). The product of hydroamination has not been observed. The different reactivity of **2a** with ammonia as compared to that with water or alcohol may be attributed to the acidity of the nucleophile. The better acidity of the coordinated water or alcohol probably facilitates the O–H bond activation. Besides, the results suggest that the addition of octahedral allenyliridium is unlikely to proceed via a highly reactive η^3 -propargyl/ η^3 -allenyl intermediate.

Recalling that the η^3 -alkoxyallyl complexes **4a** and **4b** are hydrolyzed to yield the η^3 -hydroxyallyl complex **3**, the reaction can be elucidated by an addition-elimination mechanism (Scheme 5). In other words, the alkoxyallyl complexes may be transformed into the hydroxyallyl complex via substitution at the allyl central carbon, where the entering nucleophile is a water molecule and the alcohol is the preferable leaving member. Similar reactions in the platinum systems have also been observed.¹² These substitution reactions present new chemical behavior for the η^3 -allyl complexes. A good π -donating substituent at the central η^3 -allyl carbon may prompt this carbon to be subject to

(11) (a) Burkhardt, E. R.; Doney, J. J.; Bergman, R. G.; Heathcock, C. H. *J. Am. Chem. Soc.* **1987**, *109*, 2022. (b) Slough, G. A.; Bergman, R. G.; Heathcock, C. H. *J. Am. Chem. Soc.* **1989**, *111*, 938. (c) Burkhardt, E. R.; Bergman, R. G.; Heathcock, C. H. *Organometallics* **1990**, *9*, 30. (d) Hartwig, J. F.; Bergman, R. G.; Anderson, R. A. *Organometallics* **1991**, *10*, 3326. (e) Stack, J. G.; Doney, J. J.; Bergman, R. G.; Heathcock, C. H. *Organometallics* **1990**, *9*, 453.

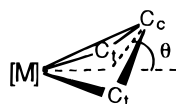
(12) Tsai, F.-Y.; Chen, H.-W.; Chen, J.-T.; Lee, G.-H.; Wang, Y. Submitted for publication.



nucleophilic attack. Such a reactivity is in contrast to the chemistry of the common η^3 -allyl complexes with nucleophiles, wherein the allyl ligand prefers to undergo attack at a terminal carbon.¹³

Utilizing the strategy of Scheme 5, we succeeded in constructing a C–N bond at the central allyl carbon. The first examples of N-protonated and N-alkylated η^3 -aza-TMM iridium complexes, $\{\text{Ir}(\text{Cl})(\text{PPh}_3)_2(\text{CO})[\eta^3\text{-CH}_2\text{C}(\text{NR}_2)\text{CH}_2]\}(\text{OTf})$ ($\text{R} = \text{H}$ (**7a**), Et (**7b**)), can thus be prepared in nearly quantitative yields by the reactions of **4a** and **4b** with NH_3 and Et_2NH , respectively (Scheme 6). Such substitution reactions serve as a pragmatic alternative methodology for C–N bond formation with metal allenyl species. The complexes **7a** and **7b** have been characterized by spectroscopy and crystallography. The X-ray structures of both **7a** and **7b** are determined. The ORTEP drawing of complex **7a** is shown in Figure 3 as being representative. The lengths of the C–N bonds in both **7a** and **7b** are in the range of substantial double-bonding. The folding angle of the MC_3 skeleton, θ , is $49.9(5)^\circ$ in **7a** and $38.9(4)^\circ$ in **7b**, which are the smallest measured values among the related species.

Structural Characteristic of Hydroxyallyl, η^3 -oxa-TMM, N-Protonated and N-Alkylated η^3 -aza-TMM Complexes. The η^3 -allyl, metallacyclobutane, and the η^3 -TMM-related complexes all have a common four-membered MC_3 skeleton. The structure of these species can be characterized by measuring the distance from the central carbon atom to the metal $D(\text{M}-\text{C}_c)$ and the dihedral angle θ defined by the $\text{C}_t-\text{C}_c-\text{C}_t$ and $\text{C}_t-\text{M}-\text{C}_t$ planes:



These structural features reflect the folding degree of the MC_3 moiety. The metallacyclobutane has a large $D(\text{M}-\text{C}_c)$ and small θ value. In fact, there is no bond between the metal and the central carbon in metallacyclobutane. An η^3 -allyl compound generally has relatively small $D(\text{M}-\text{C}_c)$ and relatively large θ . The $\text{M}-\text{C}_c$

(13) Kaduk, J. A.; Poulos, A. T.; Ibers, J. A. *J. Organomet. Chem.* **1977**, *127*, 245.

(14) Chen, J.-T.; Chen, Y.-K.; Chu, J.-B.; Lee, G.-H.; Wang, Y. Submitted for publication.

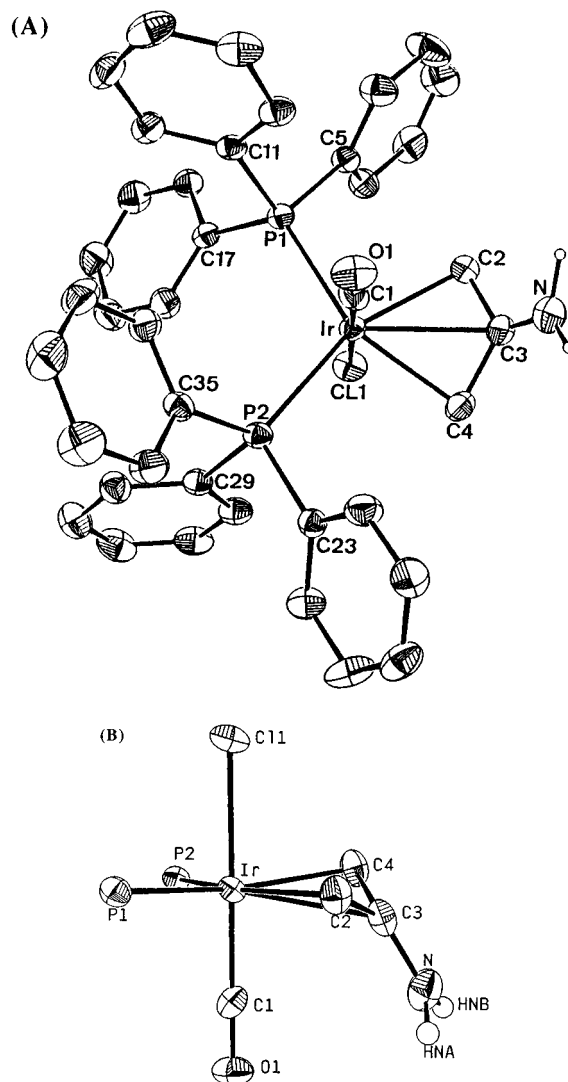


Figure 3. ORTEP drawings of the cation of **7a**, $\{\text{Ir}(\text{Cl})(\text{PPh}_3)_2(\text{CO})[\eta^3\text{-CH}_2\text{C}(\text{NH}_2)\text{CH}_2]\}^+$: (A) top view; (B) side view. All hydrogen atoms are omitted for clarity.

bond of an η^3 -allyl may be as strong as the $\text{M}-\text{C}_t$ bonds. A substituent which has a good $\text{p}\pi$ property at the allyl central carbon may cost the interaction of the $\text{M}-\text{C}_c$ bond. As a result, $D(\text{M}-\text{C}_c)$ increases and θ decreases.

Table 1 collects the characteristic structural data of several η^3 -allyl derivatives, η^3 -oxa-TMM, N-protonated and N-alkylated η^3 -aza-TMM complexes of iridium. The η^3 -2-hydroxyallyl complex **3** has a substantially longer $\text{M}-\text{C}_c$ bond and smaller θ than those of an unsubstituted allyliridium complex.¹³ The η^3 -oxa-TMM complex **5**, which contains a $\text{C}_c=\text{O}$ double bond has an even longer $D(\text{M}-\text{C}_c)$ and smaller value of θ than those of **3**. The data for $D(\text{C}_t-\text{C}_c)$ and $\angle\text{C}_t-\text{C}_c-\text{C}_t$ also support that the $\text{p}\pi-\text{p}\pi$ interaction in the $\text{C}=\text{O}$ bond occurs at the expense of the $\text{p}\pi-\text{p}\pi$ interaction in the allyl moiety. On the basis of the structural parameters, we classify **7a** to be the N-protonated η^3 -aza-TMM and **7b** to be the N-alkylated η^3 -aza-TMM complex. The η^3 -oxa-TMM and N-protonated and N-alkylated η^3 -aza-TMM derivatives may be envisaged as a class of stable intermediate species between the η^3 -allyl and metallacyclobutane groups.

Table 1. Important Structural Parameters for the MC₃ Skeleton in {Ir(Cl)(PPh₃)₂(CO)[η³-CH₂C(X)CH₂]}⁺

X	M-C _t (Å)	M-C _c (Å)	C _t -C _c (Å)	C _c -C _t -C _c (deg)	C-X (Å)	θ ^b (deg)	ref
H	2.28(1) 2.25(1)	2.24(1)	1.38(3) 1.40(3)	125(2)	1.0	65.1	13
OH	2.22 (1) 2.23(1)	2.34(1)	1.42(2) 1.40(2)	117(1)	1.33(1)	58(1)	a
O	2.169 (9) 2.184(9)	2.561(9)	1.48(2) 1.50(1)	106.6(8)	1.21(2)	41	1
NH ₂	2.182 (5) 2.203(5)	2.442(5)	1.431(7) 1.441(7)	111.6(4)	1.319(7)	49.9(5)	a
NEt ₂	2.161 (4) 2.173(4)	2.567(4)	1.457(6) 1.462(6)	106.2(3)	1.297(5)	38.9(4)	a
NMePh	2.19 (1) 2.21(1)	2.50(1)	1.40(2) 1.45(2)	110(1)	1.32(2)	47(5)	14
NPh ₂	2.15 (3) 2.18(3)	2.54(3)	1.41(4) 1.54(4)	105(2)	1.31(3)	45(5)	14

^a This work. ^b θ stands for the dihedral angle between the C_t-C_c-C_t and C_t-M-C_t planes.

Conclusions

The labile octahedral (η¹-allenyl)iridium complex (OC-6-42)-Ir(Cl)(PPh₃)₂(OTf)(CO)(η¹-CHCCH₂) undergoes regioselective C-O bond formation with water or alcohol to form the first iridium η³-2-hydroxy- and η³-2-alkoxyallyl complexes, {Ir(Cl)(PPh₃)₂(CO)[η³-CH₂C(OR)CH₂]}(OTf) (R = H, alkyl). The reaction of (OC-6-42)-Ir(Cl)(PPh₃)₂(OTf)(CO)(η¹-CHCCH₂) with ammonia yields the product of substitution {(OC-6-42)-Ir(Cl)(PPh₃)₂(NH₃)(CO)(η¹-CHCCH₂)}(OTf) instead of that of hydroamination to the allenyl ligand. These contrary results suggest that both the coordination and the acidity of the added nucleophile may be crucial to the addition to the metal η¹-allenyl species. The C-N bond formation at the central allenyl carbon can be alternatively established by the rare amino substitution for the alkoxy group at the central carbon of the η³-alkoxyallyl complexes. The products are identified to be the protonated or alkylated η³-aza-TMM iridium complexes {Ir(Cl)(PPh₃)₂(CO)[η³-CH₂C(NR₂)CH₂]}(OTf), which constitute a class of stable intermediates between the metal η³-allyl and metallacyclobutane species. The nucleophilic substitution at the central carbon of the η³-2-alkoxyallyl complexes presents chemical features new to allyl chemistry.

Experimental Section

General Considerations. The IR spectra were recorded on a Bio-Rad FTS-40 spectrophotometer. The NMR spectra were routinely measured on Bruker ACE-200 and ACE-300 spectrometers. For the ³¹P NMR spectra, spectrometer frequencies of 81.015 and 121.49 MHz were employed, respectively; chemical shifts are given in ppm (δ) relative to 85% H₃PO₄ in CDCl₃. The corresponding frequencies for ¹³C NMR spectra were at 50.32, 75.47, and 125.76 MHz for the respective spectrometers. Mass spectrometric analyses were collected on a JEOL SX-102A spectrometer. Elemental analyses were done on a Perkin-Elmer 2400 CHN analyzer.

Synthesis and Characterization. (OC-6-43)-Ir(Cl)₂(PPh₃)₂(CO)(η¹-CHCCH₂) (1a) and (OC-6-54)-Ir(Br)(Cl)(PPh₃)₂(CO)(η¹-CHCCH₂) (1b).⁴ To a dry CH₂Cl₂ solution containing *trans*-Ir(CO)(Cl)(PPh₃)₂ (485 mg) was added propargyl bromide (85% in 0.1 mL, 1.5 equiv) under dry N₂ at 0 °C. The yellow reaction solution turned to orange after 30 min. The solution was then concentrated and filtered. Introduction

of hexane/Et₂O resulted in the precipitation of a pinkish microcrystalline product in 84% yield (468 mg). For **1a**: IR (KBr pellet) ν_{C=C} 1923 cm⁻¹, ν_{CO} 2048 cm⁻¹; ³¹P NMR (CDCl₃) δ -12.8; ¹H NMR (CDCl₃) δ 3.51 (2H, dt, J_{H-H} = 6.3 Hz, J_{P-H} = 3.3 Hz, CH₂), δ 5.15 (1H, tt, J_{H-H} = 6.3 Hz, J_{P-H} = 2.5 Hz, CH), δ 7.2-7.9 (30H, m, phenyl); ¹³C NMR (CDCl₃) δ 68.2 (s, CH₂), 68.7 (t, J_{P-C} = 7.2 Hz, CH), 127-135 (phenyl), 159.7 (t, J_{P-C} = 7.2 Hz, CO), 206.5 (t, J_{P-C} = 3.5 Hz, =C=); FAB MS (*m/z*) 819.3 (M⁺ - ⁸¹Br). For **1b**: IR (KBr pellet) ν_{C=C} 1920 cm⁻¹, ν_{CO} 2055 cm⁻¹; ³¹P NMR (CDCl₃) δ -16.1; ¹H NMR (CDCl₃) δ 3.57 (2H, dt, J_{H-H} = 6.2 Hz, J_{P-H} = 3.4 Hz, CH₂), 5.31 (1H, tt, J_{H-H} = 6.2 Hz, J_{P-H} = 2.5 Hz, CH), 7.2-8.0 (30H, m, phenyl); ¹³C NMR (CDCl₃) δ 68.5 (s, CH), 70.5 (s, CH₂), 127-135 (phenyl), 159.4 (t, J_{P-C} = 8.5 Hz, CO), 206.0 (s, =C=); FAB MS (*m/z*) 901 (M⁺), 863.2 (M⁺ - ³⁷Cl), 819.2 (M⁺ - ⁸¹Br).

(OC-6-42)-Ir(Cl)(PPh₃)₂(OSO₂CF₃)(CO)(η¹-CHCCH₂) (2a). To a mixture consisting of **1b** (190 mg) and AgOTf (60 mg, 1.1 equiv) was added N₂-degassed dry CH₂Cl₂ (15 mL) at -20 °C. The solution was stirred for 30 min to allow the complete precipitation of AgBr. After AgBr was removed by filtration, the solution was concentrated. Addition of degassed dry Et₂O to the solution resulted in a whitish yellow solid product. The isolated yield of **2a** was 66% (135 mg). The elemental analysis was not acquired, for purification by recrystallization always led to decomposition. IR (KBr pellet): ν_{OTf} 1001, 1230, 1317 cm⁻¹, ν_{C=C} 1928 cm⁻¹, ν_{CO} 2063 cm⁻¹. ³¹P NMR (CDCl₃): δ -10.0. ¹H NMR (CDCl₃): δ 3.93 (2H, dt, J_{H-H} = 6.0 Hz, J_{P-H} = 4.1 Hz, CH₂), 5.66 (1H, tt, J_{H-H} = 6.0 Hz, J_{P-H} = 3.0 Hz, CH), 7.3-8.0 (30H, m, phenyl). ¹³C{¹H} NMR (CDCl₃): δ 55.2 (dt, J_{C-H} = 174 Hz, J_{P-C} = 8.5 Hz, CH), 72.4 (t, J_{C-H} = 162 Hz, CH₂), 127-135 (phenyl), 158.6 (t, J_{P-C} = 8.4 Hz, CO), 205.4 (t, J_{P-C} = 3.3 Hz, =C=).

{Ir(Cl)(PPh₃)₂(CO)(η¹-CHCCH₂)}(BF₄) (2b). Refer to the paragraph for **2a** for the synthesis; spectra were taken at -40 °C. ³¹P NMR (CDCl₃): δ -7.1. ¹H NMR (CDCl₃): δ 3.98 (2H, CH₂), 5.92 (1H, CH), 7.3-8.0 (m, phenyl). ¹³C NMR (CDCl₃): δ 51.5 (t, J_{P-C} = 6.9 Hz, CH), 72.7 (s, CH₂), 127-135 (phenyl), 157.3 (t, J_{P-C} = 6.9 Hz, CO), 206.3 (s, =C=). ¹⁹F NMR (CDCl₃, 233 K): δ -155 (s, BF₄).

{Ir(Cl)(PPh₃)₂(CO)[η³-CH₂C(OH)CH₂]}(OTf) (3). Complex **2a** was prepared in situ from **1** (140 mg) and AgOTf (45 mg, 1.1 equiv) in dry CH₂Cl₂ at -20 °C. After removal of AgBr precipitate, the filtrate was warmed to 0 °C and water was added (5.6 μL, 2.0 equiv). The reaction was allowed to continue for 30 min at 0 °C. The solution then was filtered again and concentrated. Addition of hexane provided product in 78% isolated yield (120 mg). Single crystals suitable for X-ray diffraction were grown by slowly diffusing pentane into a CH₂-Cl₂ solution of complex **3** at 5 °C. IR (KBr pellet): ν_{OTf} 1298 cm⁻¹, ν_{CO} 2048 cm⁻¹. ³¹P NMR (CDCl₃): δ -12.8. ¹H NMR (CDCl₃): δ 2.96 (2H, ddd, J_{H-H} = 4.56 Hz, J_{P-H} = 2.55, 9.51 Hz, H_{anti}), 3.78 (2H, s, br, H_{syn}), 7.3-7.6 (30H, m, phenyl), 11.54 (1H, s, OH). ¹³C NMR (CDCl₃): δ 50.4 (dd, J_{P-C} = 2.3, 40 Hz, C), 126-135 (phenyl), 159.0 (t, J_{P-C} = 8.7 Hz, CO), 168.3 (s, C).

{Ir(Cl)(PPh₃)₂(CO)[η³-CH₂C(OR)CH₂]}(OTf) (R = Me (4a), Et (4b)). Complexes **4a** and **4b** were prepared according to a procedure used for preparing **3**, except that methanol or ethanol was employed instead of water. The isolated yields were 65% for **4a** and 50% for **4b**. Recrystallization would cause decomposition. Selected spectral data for **4a**: IR (KBr pellet) ν_{OTf} 1266 cm⁻¹, ν_{CO} 2052 cm⁻¹; ³¹P NMR (CDCl₃) δ -13.9; ¹H NMR (CDCl₃) δ 3.16 (2H, dd, J_{H-P} = 8.7 Hz, H_{anti}), 3.60 (2H, s, br, H_{syn}), 3.78 (3H, s, OCH₃), 7.3-7.7 (30H, m, phenyl); ¹³C NMR (CDCl₃) δ 48.8 (d, J_{P-C} = 40 Hz, C), 75.6 (s, OCH₃), 127-134 (phenyl), 159.0 (t, J_{P-C} = 8.4 Hz, CO), 168.1 (s, C). For **4b**: IR (KBr pellet) ν_{OTf} 1266 cm⁻¹, ν_{CO} 2045 cm⁻¹; ³¹P NMR (CDCl₃) δ -14.0; ¹H NMR (CDCl₃) δ 1.34 (3H, t, J_{H-H} = 6.9 Hz, CH₃), 3.15 (2H, dd, J_{H-P} = 6.7 Hz, H_{anti}), 3.58 (2H, s, br, H_{syn}), 3.97 (2H, q, J_{H-H} = 6.9 Hz, CH₂CH₃), 7.3-7.6 (30H, m, phenyl); ¹³C NMR (CDCl₃) δ 13.7 (s,

Table 2. X-ray Crystal Parameters and Data Collection Details for Complexes 3, 6, 7a, and 7b

	3	6	7a	7b
formula	C ₄₁ H ₃₅ O ₅ P ₂ SF ₃ IrCl·CH ₂ Cl ₂	C ₄₁ H ₃₇ O ₆ P ₂ SF ₃ IrCl·CH ₂ Cl ₂	C ₄₁ H ₃₆ NO ₄ P ₂ SF ₃ IrCl·CH ₂ Cl ₂	C ₄₅ H ₄₄ NO ₄ P ₂ SF ₃ IrCl·CH ₂ Cl ₂
fw	1071.34	1089.36	1070.36	1126.47
cryst dimens, mm	0.1 × 0.15 × 0.35	0.03 × 0.25 × 0.25	0.15 × 0.4 × 0.45	0.2 × 0.5 × 0.5
space group	<i>P</i> $\bar{1}$	<i>P</i> $\bar{1}$	<i>P</i> $\bar{1}$	<i>P</i> $\bar{1}$
<i>a</i> , Å	10.060(5)	11.099(2)	12.842(3)	12.502(2)
<i>b</i> , Å	15.030(2)	11.627(2)	12.989(3)	13.051(3)
<i>c</i> , Å	15.355(2)	18.659(4)	13.589(5)	15.781(2)
α , deg	111.69(1)	88.36(2)	89.85(2)	105.69(2)
β , deg	98.01(2)	88.53(2)	92.98(3)	89.85(1)
γ , deg	89.02(2)	67.814(2)	106.66(2)	109.43(2)
<i>V</i> , Å ³	2135(1)	2228.5(8)	2168(1)	2326.9(7)
<i>Z</i>	2	2	2	2
ρ (calcd), Mg m ⁻³	1.665	1.623	1.639	1.542
<i>F</i> (000)	1088	1078	976	1040
radiation, λ , Å	Mo K α , 0.7107	Mo K α , 0.7107	Mo K α , 0.7107	Mo K α , 0.7107
<i>T</i> , K	298	298	298	298
μ , mm ⁻¹	3.36	3.34	3.30	3.08
transmissn	0.78–1.0	0.78–1.0	0.75–1.0	0.57–1.0
max 2 θ , deg	45	45	50	50
hkl	±10,16,±15	±11,12,±20	±15,15,±16	±13,15,±18
no. of rflns measd	5584	5836	7632	8202
no. of rflns obsd	4801 (>2.0 σ)	4385 (>2.0 σ)	6446 (>2.0 σ)	7214 (>2.0 σ)
no. of variables	451	523	539	551
<i>R</i> (<i>F</i>)	0.048	0.062	0.031	0.029
<i>R</i> _w (<i>F</i>)	0.060	0.062	0.026	0.023
<i>S</i>	1.10	3.01	1.95	2.23
(Δ / σ) _{max}	0.006	0.027	0.042	0.019

Table 3. Selected Bond Distances (Å) and Angles (deg)

{Ir(Cl)(PPh₃)₂(CO)[η^3-CH₂C(OH)CH₂]}(OTf) (3)							
Ir–Cl(1)	2.370(3)	Ir–C(1)	1.86(1)	Ir–C4	2.23(1)	C3–C4	1.40(2)
Ir–P1	2.395(3)	Ir–C2	2.22(1)	C1–O1	1.11(1)	C3–O2	1.33(1)
Ir–P2	2.389(3)	Ir–C3	2.34(1)	C2–C3	1.42(2)		
Cl1–Ir–P1	91.5(1)	P1–Ir–C2	156.1(3)	C1–Ir–C2	95.0(5)	Ir–C3–C2	67.2(6)
Cl1–Ir–P2	82.7(1)	P1–Ir–C3	122.3(3)	C1–Ir–C3	81.4(5)	Ir–C3–C4	67.9(6)
Cl1–Ir–C1	176.0(4)	P1–Ir–C4	90.6(3)	C1–Ir–C4	96.7(5)	Ir–C3–O2	122.3(8)
Cl1–Ir–C2	85.8(3)	P2–Ir–C1	93.4(4)	C2–Ir–C3	36.2(4)	C2–C3–C4	117(1)
Cl1–Ir–C3	101.4(3)	P2–Ir–C2	90.7(3)	C2–Ir–C4	65.6(4)	C2–C3–O2	122(1)
Cl1–Ir–C4	87.2(3)	P2–Ir–C3	124.8(3)	C3–Ir–C4	35.6(4)	C4–C3–O2	119(1)
P1–Ir–P2	112.5(1)	P2–Ir–C4	154.9(3)	Ir–C1–O1	178(1)	Ir–C4–C3	76.5(7)
P1–Ir–C1	89.3(4)			Ir–C2–C3	76.6(6)		
(OC-6-52)-{Ir(Cl)(PPh₃)₂(H₂O)(CO)[η^1-CH₂C(O)CH₃]}(OTf) (6)							
Ir–Cl(1)	2.458(4)	Ir–C(1)	1.76(2)	Ir–O2	2.10(1)	C3–C4	1.63(3)
Ir–P1	2.433(4)	Ir–C2	2.13(2)	C1–O1	1.18(2)	C3–O3	1.17(2)
Pt–P2	2.415(5)			C2–C3	1.58(3)		
Cl1–Ir–P1	87.0(2)	P1–Ir–P2	178.6(2)	C1–Ir–C2	100.4(7)	Ir–C2–C3	111(1)
Cl1–Ir–P2	94.2(2)	P1–Ir–C1	91.8(5)	P2–Ir–C2	89.9(4)	C2–C3–C4	105(2)
Cl1–Ir–C1	86.1(5)	P1–Ir–C2	88.8(4)	P2–Ir–O2	92.3(3)	C2–C3–O3	131(2)
Cl1–Ir–C2	172.4(5)	P1–Ir–O2	87.1(3)	C2–Ir–O2	85.0(5)	C4–C3–O3	124(2)
Cl1–Ir–O2	88.4(3)	P2–Ir–C1	88.9(5)	Ir–C1–O1	175(1)	C1–Ir–O2	174.5(6)
{Ir(Cl)(PPh₃)₂(CO)[η^3-CH₂C(NH₂)CH₂]}(OTf) (7a)							
Ir–Cl(1)	2.385(1)	Ir–C(1)	1.836(5)	Ir–C4	2.203(5)	C3–C4	1.441(7)
Ir–P1	2.394(2)	Ir–C2	2.182(5)	C1–O1	1.144(6)	C3–N	1.319(7)
Ir–P2	2.417(1)	Ir–C3	2.442(5)	C2–C3	1.431(7)		
Cl1–Ir–P1	84.00(5)	P1–Ir–C2	90.5(1)	C1–Ir–C2	94.0(2)	Ir–C3–C2	62.3(3)
Cl1–Ir–P2	93.5(5)	P1–Ir–C3	124.5(1)	C1–Ir–C3	81.1(2)	Ir–C3–C4	63.1(3)
Cl1–Ir–C1	179.6(2)	P1–Ir–C4	154.2(1)	C1–Ir–C4	95.6(2)	Ir–C3–N	130.0(4)
Cl1–Ir–C2	86.3(1)	P2–Ir–C1	86.3(1)	C2–Ir–C3	35.5(2)	C2–C3–C4	111.6(4)
Cl1–Ir–C3	99.4(1)	P2–Ir–C2	159.1(1)	C2–Ir–C4	65.6(2)	C2–C3–N	123.7(4)
Cl1–Ir–C4	84.8(2)	P2–Ir–C3	124.6(1)	C3–Ir–C4	35.7(2)	C4–C3–N	122.1(5)
P1–Ir–P2	110.24(5)	P2–Ir–C4	93.6(1)	Ir–C1–O1	179.0(4)	Ir–C4–C3	81.2(3)
P1–Ir–C1	95.7(2)			Ir–C2–C3	82.2(3)		
{Ir(Cl)(PPh₃)₂(CO)[η^3-CH₂C(NEt₂)CH₂]}(OTf) (7b)							
Ir–Cl(1)	2.395(1)	Ir–C2	2.173(4)	C5–N	1.470(6)	C3–C4	1.462(6)
Ir–P1	2.424(1)	Ir–C3	2.161(4)	C7–N	1.487(6)	C5–C6	1.509(7)
Ir–P2	2.438(1)	Ir–C4	2.567(4)	C1–O1	1.132(5)	C7–C8	1.489(7)
Ir–C(1)	1.827(4)	C4–N	1.297(5)	C2–C4	1.457(6)		
Cl1–Ir–P1	85.95(4)	P1–Ir–C3	91.3(1)	C2–Ir–C3	65.2(2)	Ir–C4–C2	57.7(2)
Cl1–Ir–P2	92.88(4)	P1–Ir–C4	124.8(9)	C1–Ir–C4	34.5(2)	Ir–C4–C3	57.3(2)
Cl1–Ir–C1	177.3(1)f	P2–Ir–C1	87.2(1)	C3–Ir–C4	34.7(1)	Ir–C4–N	143.7(3)
Cl1–Ir–C2	85.4(1)	P2–Ir–C2	95.0(1)	C4–N–C5	122.3(4)	C2–C4–C3	106.2(3)
Cl1–Ir–C3	86.5(1)	P2–Ir–C3	160.2(1)	C4–N–C7	122.1(3)	C2–C4–N	126.8(4)
Cl1–Ir–C4	97.52(9)	P2–Ir–C4	126.29(9)	C5–N–C7	115.5(3)	C3–C4–N	125.7(4)
P1–Ir–P2	108.40(4)	C1–Ir–C2	92.0(2)	Ir–C1–O1	176.4(3)	N–C5–C6	111.7(4)
P1–Ir–C1	96.6(1)	C1–Ir–C3	92.6(2)	Ir–C2–C4	87.7(2)	N–C7–C8	111.9(4)
P1–Ir–C2	155.4(1)	C1–Ir–C4	80.3(1)	Ir–C3–C4	88.0(2)		

OCH₂CH₃), 49.0 (d, $J_{P-C} = 40$ Hz, C_i), 67.2 (s, OCH₂), 127–134 (phenyl), 159.3 (t, $J_{P-C} = 8.6$ Hz, CO), 167.9 (s, C_j).

Ir(Cl)(PPh₃)₂(CO)[η^3 -CH₂C(O)CH₂] (5).¹ To CDCl₃ (1 mL) containing **3** (30 mg) was added Et₃N (5 μ L) at 25 °C. The solution was stirred for 10 min. A white solid in 71% yield (19 mg) was recovered by recrystallization. ³¹P NMR (CDCl₃): δ -10.5. ¹H NMR (CDCl₃): δ 2.47 (2H, m, $J_{H-H} = 7.9$ Hz, CH₂), 2.62 (2H, t, $J_{H-H} = 7.9$ Hz). ¹³C NMR (CDCl₃): δ 37.1 (s, C_i), 127–135 (phenyl), 164.4 (t, $J_{P-C} = 4.0$ Hz, CO), 197.2 (s, C_j).

(OC-6-52)-{Ir(Cl)(PPh₃)₂(H₂O)(CO)[η^1 -CH₂C(O)CH₃]}-(OTf) (6). Complex **4a** or **4b** was left in solution under ambient conditions for days. A grayish solid product was precipitated by introducing hexane into the solution. The isolated yield was 70%. Single crystals suitable for X-ray diffraction were grown by slowly diffusing pentane into a CH₂Cl₂ solution of complex **6** at 5 °C. IR (KBr pellet): ν_{OTf} 1295 cm⁻¹, ν_{CO} 1698, 2050 cm⁻¹. ³¹P NMR (CDCl₃): δ 4.7. ¹H NMR (CDCl₃): δ 1.29 (3H, s, CH₃), 3.13 (2H, t, $J_{P-H} = 3.8$ Hz, CH₂), 5.63 (2H, s, H₂O), 7.3–7.6 (30H, m, phenyl). ¹³C NMR (CDCl₃): δ 27.4 (s, CH₃), 29.4 (t, $J_{P-C} = 3.4$ Hz, CH₂), 127–135 (phenyl), 158.5 (t, $J_{P-C} = 10.4$ Hz, terminal CO), 210.8 (s, enolate CO).

{Ir(Cl)(PPh₃)₂(CO)[η^3 -CH₂C(NR₂)CH₂]}(OTf) (R = H (7a), Et (7b)). To a degassed dry CH₂Cl₂ solution containing **4a** (90 mg) was added concentrated NH₄OH (6.0 μ L, 2 equiv of NH₃). After 15 min of stirring, the solution was concentrated to precipitate a light green product. The isolated yield was 70%. **7b** was prepared from **4a** (or **4b**) and Et₂NH by a similar procedure. Single crystals suitable for X-ray diffraction were grown by slowly diffusing pentane into a CH₂Cl₂ solution of either **7a** or **7b** at 5 °C. Selected spectral data for **7a**: IR (KBr pellet) ν_{OTf} 1284 cm⁻¹, $\nu_{C=N}$ 1640 cm⁻¹, ν_{CO} 2048 cm⁻¹; ³¹P NMR (CDCl₃) δ -12.6; ¹H NMR (CDCl₃) δ 2.52 (2H, dd, $J_{H-H} = 7.4$ Hz, $J_{H-P} = 10.1$ Hz, H_{anti}), 3.01 (2H, s, br, H_{syn}), 7.07 (2H, s, NH₂), 7.2–7.4 (30H, m, phenyl); ¹³C NMR (CDCl₃) δ 34.3 (dd, $J_{P-C} = 2.4$, 52.5 Hz, C_i) 128–134 (phenyl), 161.4 (t, $J_{P-C} = 8.2$ Hz, CO), 172.8 (t, $J_{P-C} = 3.1$ Hz, C_j). Anal. Calcd for IrC₄₁H₃₆O₄ClNP₂SF₃: C, 50.00; H, 3.68. Found: C, 49.30; H, 3.55. For **7b**: IR (KBr pellet) ν_{OTf} 1271 cm⁻¹, $\nu_{C=N}$ 1606 cm⁻¹, ν_{CO} 2030 cm⁻¹; ³¹P NMR (CDCl₃) δ -12.5; ¹H NMR (CDCl₃) δ 1.08 (6H, t, $J_{H-H} = 7.3$ Hz, CH₃ (Et)), 2.19 (2H, d, $J_{H-H} = 10.0$ Hz, H_{anti}), 2.59 (2H, dd, $J_{H-H} = 10.0$ Hz, $J_{H-P} = 5.3$ Hz, H_{syn}), 3.36 (4H, tq, $J_{H-H} = 7.3$ Hz, $J_{H-P} = 16.0$ Hz, CH₂ (Et)), 7.3–7.5 (30H, m, phenyl); ¹³C NMR (CDCl₃) δ 11.5 (s, CH₃ (Et)), 16.4 (d, $J_{P-C} = 58.6$ Hz, C_i), 45.5 (s, CH₂CH₃), 128–134 (phenyl), 163.2 (t, $J_{P-C} = 8.2$ Hz, CO), 182.7 (s, C_j).

(OC-6-42)-{Ir(Cl)(PPh₃)₂(NH₃)(CO)(η^1 -CHCCH₂)}-(OTf) (8). To a mixture containing **1b** (250 mg, 0.28 mmol) and AgOTf (1.1 equiv) was added 15 mL of N₂-degassed dry CH₂Cl₂ at -30 °C followed by NH₄OH (32 μ L, 1 equiv). The reaction solution was stirred at 0 °C for 1 h. After AgBr was removed by filtration, the reaction solution was concentrated. The addition of degassed dry Et₂O to the solution resulted in a yellow solid product. The isolated yield of **8** was 70% (126 mg) after recrystallization. IR (KBr pellet): $\nu_{C=C}$ 1925 cm⁻¹, ν_{CO} 2070 cm⁻¹. ³¹P NMR (CDCl₃): δ -14.0. ¹H NMR (CDCl₃): δ 2.76 (3H, br, NH₃), 3.67 (2H, dt, $J_{H-H} = 6.4$ Hz, $J_{P-H} = 3.7$ Hz, CH₂), 6.10 (1H, tt, $J_{H-H} = 6.4$ Hz, $J_{P-H} = 2.8$ Hz, CH), 7.2–8.0 (30H, m, phenyl). ¹³C NMR (CDCl₃): δ 56.1 (t, $J_{P-C} = 7.8$ Hz, CH), 69.2 (s, CH₂), 118–135 (phenyl), 157.4 (t, $J_{P-C} = 7.4$ Hz, CO), 208.0 (s, =C=). FAB MS (m/z) 819.4 (M⁺). Anal. Calcd for IrC₄₃H₄₀O₄ClNP₂SF₃: C, 49.94; H, 3.68; N, 1.42. Found: C, 49.52; H, 3.68; N, 1.14.

X-ray Crystallographic Analysis. Diffraction data were measured at 298 K on a Nonius CAD-4 diffractometer with graphite-monochromatized Mo K α radiation. Cell parameters were determined by a least-squares fit on 25 reflections. Intensity data were corrected for absorption on the basis of an experimental ψ rotation curve. The refinement procedure was by a full-matrix least-squares method, including all the non-hydrogen atoms anisotropically. Hydrogen atoms were fixed at the ideal geometry and a C–H distance of 1.0 Å; their isotropic thermal parameters were fixed to the values of the attached carbon atoms at the convergence of the isotropic refinement. Atomic scattering factors were taken from ref 15. Computing programs are from the NRCC SDP VAX package.¹⁶ Crystallographic data and selected bond parameters of **3**, **6**, **7a**, and **7b** are collected in Tables 2 and 3, respectively. Other detailed data are supplied in the Supporting Information.

Acknowledgment. We thank the National Science Council, Taiwan, ROC, for financial support.

Supporting Information Available: Fully labeled ORTEP drawings and tables giving complete crystal data, complete bond lengths and angles, atomic coordinates, and thermal parameters for **3**, **6**, **7a**, and **7b** (32 pages). Ordering information is given on any current masthead page.

OM960261A

(15) *International Tables for X-ray Crystallography*; Kynoch Press: Birmingham, U.K., 1974; Vol. IV.

(16) NRC VAX: Gabe, E. J.; LePage, Y.; Charland, J.-P.; Lee, F. L.; White, P. S. *J. Appl. Crystallogr.* **1989**, *22*, 384.